Proceedings of the 20th International Conference on Soil Mechanics and Geotechnical Engineering– Rahman and Jaksa (Eds)
© 2022 Australian Geomechanics Society, Sydney, Australia, ISBN 978-0-9946261-4-1

Structure of cemented granular materials

Tejas G. Murthy & Saurabh Singh
Department of Civil Engineering, Indian Institute of Science, India, tejas@iisc.ac.in

ABSTRACT: We present an exercise in quantification of cemented granular materials using x-ray computed tomography. Two model material systems, sand-epoxy and sand-cement, were used. The contact bound specimens (cemented granular materials with cementation only at the contacts) with different dimensions and average particle sizes were prepared and scanned in x-ray computed tomograph. The reconstructed scan volumes were segmented using a modified watershed segmentation algorithm for particles and contacts - where cementation resides. A network of particle was constructed and coordination number distribution for different specimens was extracted. The three-dimensional scatter plots of coordination number along with their statistical distributions are presented in this article. For the segmented particles, equivalent ellipsoids (identical second moment of inertia matrix) were used to estimate the orientation and size of the particles. For contacts, using principal component analysis, the direction of normal was extracted. We present the directional distribution of major particle orientation and contact normal with a three-dimensional rose diagram or spherical histogram. Further, contact normal and particle fabric tensors were also extracted in this exercise. We further present the particle and contact fabric tensor as a three-dimensional field of fabric tensors where fabric tensors are plotted as ellipsoids.

RÉSUMÉ : Nous présentons un exercice de quantification de matériaux granulaires cimentés par tomodensitométrie aux rayons X. Deux systèmes de matériaux modèles, sable-époxy et sable-ciment, ont été utilisés. Les échantillons liés par contact (matériaux granulaires cimentés avec cémentation uniquement au niveau des contacts) avec différentes dimensions et tailles de particules moyennes ont été préparés et scannés dans une tomographie par rayons X. Les volumes de numérisation reconstruits ont été segmentés à l'aide d'un algorithme de segmentation modifié des bassins versants pour les particules et les contacts - là où réside la cimentation. Un réseau de particules a été construit et la distribution des numéros de coordination pour différents spécimens a été extraite. Les diagrammes de dispersion en trois dimensions du nombre de coordination ainsi que leurs distributions statistiques sont présentés dans cet article. Pour les particules segmentées, des ellipsoïdes équivalents (matrice de deuxième moment d'inertie identique) ont été utilisés pour estimer l'orientation et la taille des particules. Pour les contacts, en utilisant l'analyse en composantes principales, la direction de la normale a été extraite. Nous présentons la distribution directionnelle de l'orientation des particules majeures et de la normale de contact avec un diagramme de rose en trois dimensions ou un histogramme sphérique. En outre, des tenseurs de contact normal et de tissu de particules ont également été extraits dans cet exercice. Nous présentons en outre le tenseur de tissu de particules et de contact comme un champ tridimensionnel de tenseurs de tissu où les tenseurs de tissu sont représentés sous forme d'ellipsoïdes.

KEYWORDS: x-ray computed tomography, cemented granular materials, fabric ellipsoids, fabric chains.

1 INTRODUCTION

Macroscopic behavior of cemented granular material is a function of its structure, i.e., overall arrangement of particle and bonds – also referred as "fabric" (Oda 1982, Oda et. al. 1982, Burland 1990, Coop and Atkinson 1993, Cuccovillo and Coop 1999). In cemented granular materials, the ratio of cement (binder) to the particle (volumetric or gravimetric) content controls this geometric arrangement (Sowers and Sowers 1951).

At low binder content, a "contact bound structure" is formed such that the binder exists only at the contacts. At a relatively higher binder content, a matrix bound structure is formed where particles are sparsely distributed in the matrix of binder. To extract the structure of granular materials, x-ray computed tomography has been used extensively (Ando et. al. 2012, Druckery et. al. 2016, Fonseca et. al. 2012, Singh et. al. 2020). A detailed geometric description of the granular ensemble can be obtained using segmentation algorithms such as watershed technique. From these descriptions, we can characterize the structure of granular ensemble with coordination number, fabric tensor, and spherical histograms.

In this study, we characterize the structure of cemented granular material with coordination number histogram, fabric tensors, and spherical histograms.

2 EXPERIMENTS AND IMAGE ANALYSIS

A series of XCT scans were performed on a model cemented granular material with contact bound structure -- sand cemented with epoxy. The contact bound structure was prepared with epoxy bridging the network of sand particle, i.e., epoxy bond existed only at the contact of sand particles. The epoxy binder is prepared by mixing the epoxy resin (Lapox L-12, density 1.1-1.2g/cm^3, viscosity 9000-12000centipoise) with hardener (Lapox K-6, density 1.1g/cm^3, viscosity 5-15centipoise) at weight ratio of 10:1.

Table 1. Experimental matrix for cylindrical epoxy cemented sand specimen. D – specimen diameter, height/diameter – 2, D_p – particle diameter, Res. – resolution, N_p – number of particles, CN – coordination number.

Label	D (mm)	D_p (mm)	Res.	N_p	CN
SP10	10	2.1	12.5	45	5.42
SP11	10	1.1	12.2	531	7.02
SP12	10	0.3	12.4	20289	6.04
SP13	20	2.4	25.3	591	6.49
SP14	20	1.2	25.3	7432	7.14
SP15	20	0.4	25.0	113545	6.24
SP16	38	2.5	46.3	6245	7.42
SP17	38	1.0	48.1	55961	5.64

To achieve a contact bound structure, sand was mixed with epoxy binder (2% binder content by weight of the solid particles or sand); the mixture was poured and compacted in a cylindrical mold in three layers. The specimen along with the mold is oven dried at 50^{o}C for 24 hours: it achieves sufficient strength in 24 hours to stand by itself. The specimen is extracted from the mold and oven dried at same temperature until the weight becomes constant. Specimens of different sizes were prepared with sands of varying particle sizes to investigate the effect of specimen and particle size on the structure of contact bound cemented granular materials (table 1). Figure 1 shows the grain size distribution of each specimen used in this study.

The prepared specimens are then scanned in x-ray computed tomography setup. The scanned images were segmented using a hybrid-watershed algorithm provided in Singh 2020.

The matrix of specimens used in this study is provided in the table 1.

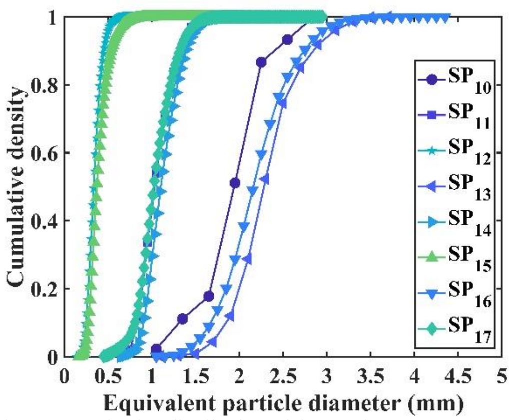

Figure 1. Grain size distribution of the specimens.

3 RESULTS AND DISCUSSION

All the specimens are segmented for sand particles and contacts. The network of sand particles is constructed by joining the center of bonded sand particles. Figure 2 shows a typical network of cemented sand specimen. The violet color dots represent the particle centroids and black lines joining them are representation of their connectivity. The coordination number and other characteristics are evaluated from the network and are presented in ensuing.

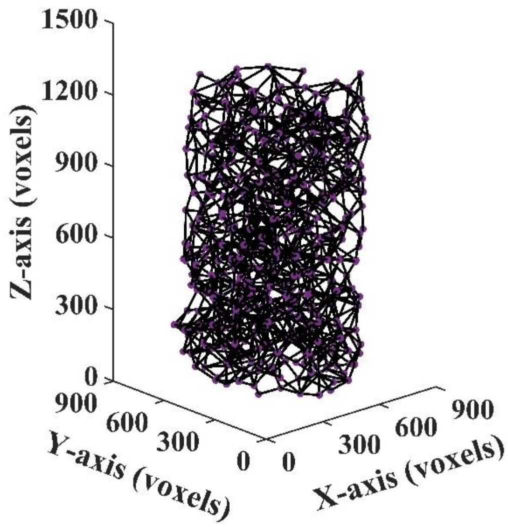

Figure 2. A typical network of contact bound cemented granular material with sand particle as node and epoxy bond as a bridge.

Figure 3 shows the spatial distribution of coordination number of sand particles. In a cemented sand specimen, two adjacent particles have multiple contacts; however, there multiple contacts are only accounted as one connection. The coordination number accounts for number of connections rather than the actual number of contacts. The coordination number ranges from two to thirteen; the most frequent coordination number lies in the range of five to seven (figure 4). The coordination number is affected by the boundary of the specimen (figure 3): only internal particles are accounted for calculation of coordination number histogram.

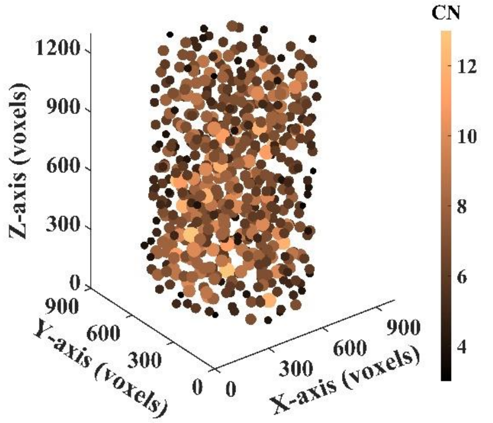

Figure 3. Spatial distribution of coordination number of sand particles.

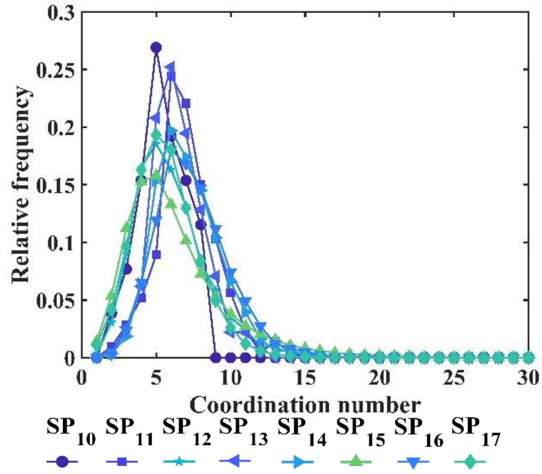

Figure 4. Histogram of internal coordination number for each specimen.

Figure 5 presents the distribution of average coordination number along vertical, radial, and circumferential directions. A set of bins along these directions were considered and average coordination number of particles in those bins is calculated. The coordination number distribution is more uniform along circumferential direction than radial and vertical. The number of particles in specimen SP_1 are fewer than required to satisfy continua: the average coordination number profile is distinct from other specimens.

The anisotropy of a granular ensemble is measured with fabric tensor associated to contact normals and particles. These fabric tensors are calculated and represented using the ellipsoids such that the major, intermediate, and minor axis of fabric ellipsoids are oriented along the corresponding eigenvectors of fabric tensor. In figure 6, we present the contact and particle fabric ellipsoids for a typical specimen; each ellipsoid is scaled in a way that the major axis of ellipsoids matches corresponding particle size. Particle fabric ellipsoids provide the orientation of particles and contact fabric ellipsoids direct themselves along the directions in which contact normal density is optimum.

Figure 7 presents the vertical component of dominant eigenvector associated with contact and particle fabric tensors of each particle of all the specimen. For all the specimen, contact normals have a tendency to direct themselves along the vertical direction, i.e., the maximum frequency of particles for dominant eigenvector of contact normal fabric is associated to zcomponent of 0.8-1 (along the z-direction). The particles have a tendency to align themselves away from the vertical axis, i.e., along the horizontal plane.

This observation is further affirmed with the directional distribution of contact normal and particle orientation in figure 8.

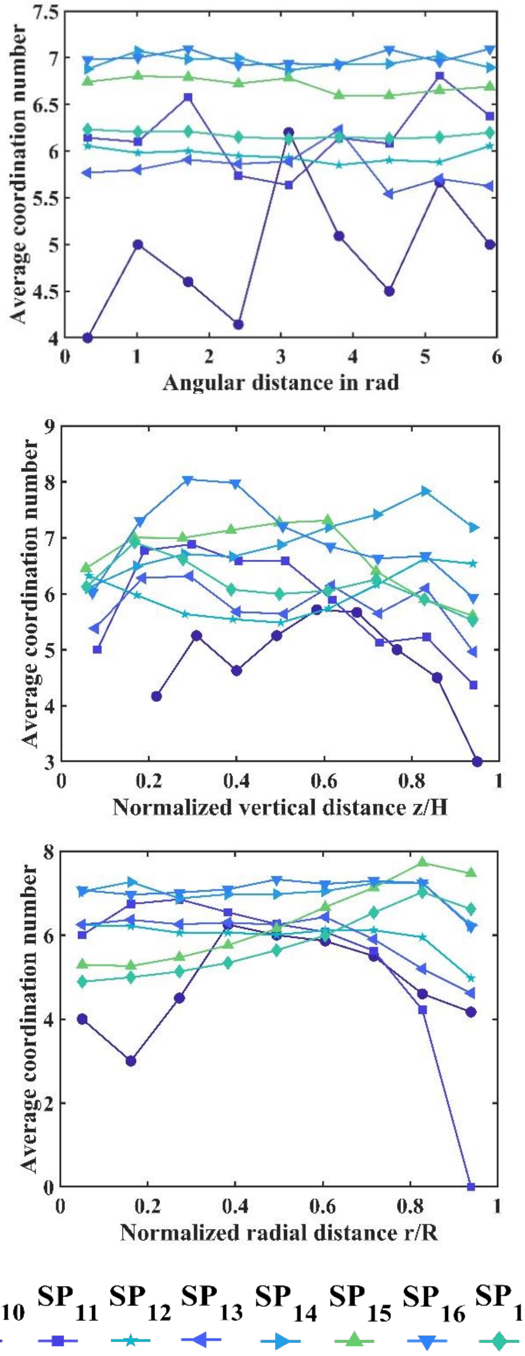

Figure 5. Coordination number distributions along circumferential, vertical and radial directions.

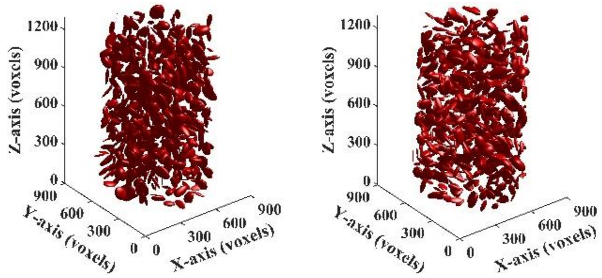

Figure 6. Contact and particle fabric ellipsoids for sand-epoxy specimen.

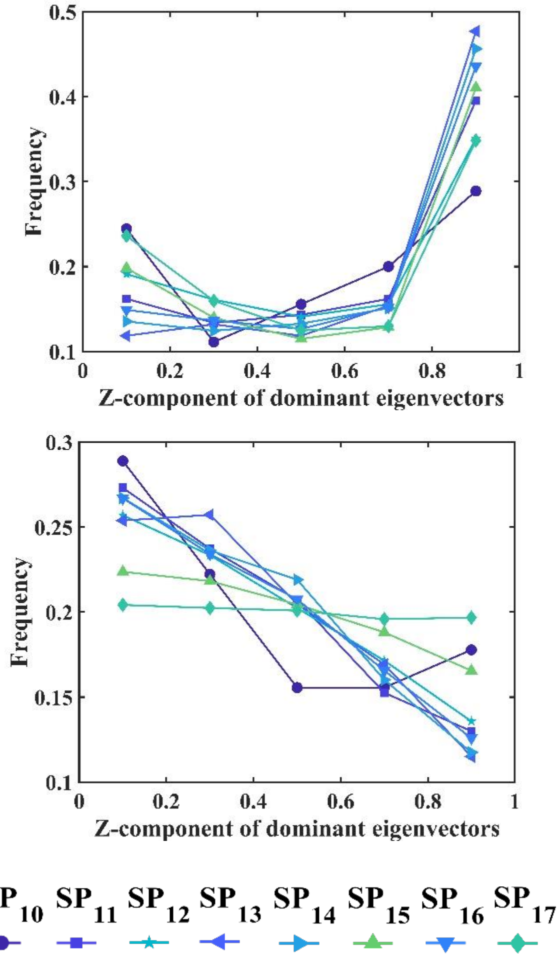

Figure 7. The vertical component of dominant eigenvector of contact normal and particle fabric tensor.

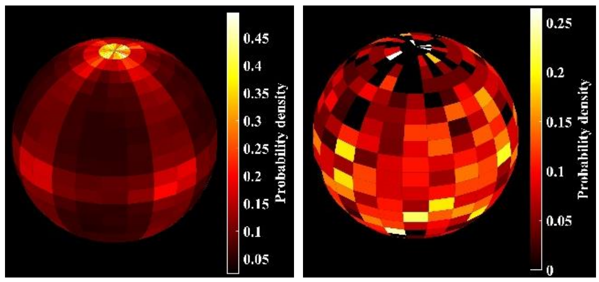

Figure 8. Directional distribution of contact normal and major particle orientation presented on the surface of unit sphere for SP_{13}.

4 CONCLUSIONS

A set of sand-epoxy specimen was studied using x-ray computed tomography. The networks of all these specimens were extracted and distribution of coordination number within the specimen was analyzed. The average coordination number lies between 6-8. The coordination number is uniform along circumferential direction more than radial and vertical directions. Further, contact normal and particle fabric tensors are evaluated for each particle and are presented as fabric ellipsoids. The major eigenvectors of these fabric tensor points towards the direction of maximum contact normal density and particle orientation. These dominant eigenvectors were further analyzed: the particles orient themselves normal to the direction of gravity and contact normals orient themselves towards the direction of gravity. This is further affirmed using directional distribution of contact normal and particle orientation in a three-dimensional spherical histogram.

5 ACKNOWLEDGEMENT

The authors would like to thank Dr. John C. Miers and Prof. Christopher J. Saldana. This research work was funded by the Science and Engineering Research Board, India.

6 REFERENCES

Andò E., Hall S. A., Viggiani G., Desrues J., and Bésuelle P. (2012). Experimental micromechanics: grain-scale observation of sand deformation. Géotechnique Letters, 2(3), 107–112.

Burland J. B. (1990). On the compressibility and shear strength of natural clays. Géotechnique, 40(3), 329–378.

Coop, M. R. and Atkinson, J. H. (1993). The mechanics of cemented carbonate sands. Geotechnique, 43(1), 53–67.

Cuccovillo, T. and Coop, M. R. (1999). On the mechanics of structured sands. Géotechnique, 49(6), 741–760.

Druckrey A. M., Alshibli K. A., and Al-Raoush R. I. (2016). 3D characterization of sand particle-to-particle contact and morphology. Computers and Geotechnics, 74, 26–35.

Fonseca J., O'Sullivan C., Coop M. R., and Lee P. D. (2012). Non-invasive characterization of particle morphology of natural sands. Soils and Foundations, 52(4), 712 – 722.

Oda M. (1982). Fabric tensor for discontinuous geological materials. Soils and Foundations, 22(4), 96–108.

Oda M., Nemat-Nasser S., and Mehrabadi M. M. (1982). A statistical study of fabric in a random assembly of spherical granules. International Journal for Numerical and Analytical Methods in Geomechanics, 6(1), 77–94.

Singh S., Miers J.C., Saldana C., and Murthy T.G., (2020). Quantification of fabric in cemented granular materials. Computers and Geotechnics, Vol. 125, pp. 103644.

Singh S. (2020). Weakly cemented granular materials: study at multiple length scales. PhD thesis, IISc Bangalore.

Sowers G. B. and Sowers G. F. (1951). Introductory soil mechanics and foundations, volume 72. LWW.